Inorg. Chem. **2006**, *45*, 4987–4995

Inorganic Chemistry
Article

Transformation from a Low-Dimensional Framework to a High-Dimensional Architecture Based on Different Metal Ions: Syntheses, Structures, and Photoluminescences

Yun Gong,[†,‡] Wang Tang,[†] Wenbin Hou,[§] Zhongyong Zha,[§] and Changwen Hu*,[†]

Department of Chemistry, Beijing Institute of Technology, Beijing 100081, P. R. China,
Department of Applied Chemistry, Chongqing University, Chongqing 400044, P. R. China, and
Department of Chemistry, Logistical Engineering University, Chongqing 400016, P. R. China

Received December 8, 2005

Five novel metal pamidronates (3-ammonium-1-hydroxypropylidene-1,1-bisphosphonate, APD) formulated as $Ni_2(C_3NH_{10}P_2O_7)_4 \cdot 4H_2O$ (**1**), $M(C_3NH_9P_2O_7) \cdot H_2O$ (M = Co (**2**), Mn (**3**), Zn (**4**)) and $Cu_3(C_3NH_8P_2O_7)_2 \cdot 2H_2O$ (**5**) have been hydrothermally synthesized under similar conditions. Compound **1** is a molecular binuclear nickel cluster. Compounds **2** and **3** exhibit similar one-dimensional ladderlike structures. Compound **4** possesses a novel two-dimensional gridlike framework. Compound **5** shows an unusual three-dimensional architecture, in which two-dimensional layers with a parquet motif are pillared by $\{CuO_4\}$ planar squares. Different dinuclear secondary building units (SBUs) are observed in compounds **1**–**5**, depending on the different coordination modes of APD. They also exhibit different photoluminescence properties.

Introduction

Organic−inorganic hybrids constitute an important class of compounds in advanced materials design.[1] In the rational design and synthesis of organic−inorganic hybrids, certain factors are always taken into account, such as the coordination nature of the metal ion, the functionality, flexibility, and symmetry of the organic ligands, and the template effect of structure-directing agents.[2]

Metal organophosphonates represent a particularly versatile field due to their wide variety of accessible structure types and their potential application in areas such as ion exchange, catalysis, and nonlinear optics.[3] Consequently, a variety of metal organophosphonates with interesting compositions and topologies have been prepared.[4,5] However, organophosphonate materials containing divalent transition metal cations are most often lamellar in nature.[4] The metal ions are bridged by the phosphonate groups to form an inorganic hydrophilic layer, and the remaining organic part of the organophosphonate generally dangles in the interlayer region. Organodiphosphonic acids such as $H_2O_3P(CH_2)_nPO_3H_2$ ($n \geq 1$) are usually used to construct three-dimensional architectures because their organic parts can act as covalently bonded

---

* To whom correspondence should be addressed. E-mail: cwhu@bit.edu.cn.

[†] Beijing Institute of Technology.

[‡] Chongqing University.

[§] Logistical Engineering University.

(1) (a) Moulton, B.; Zaworotko, M. J. *Chem. Rev.* **2001**, *101*, 1629. (b) Cantrill, S. J.; Chichak, K. S.; Peters, A. J.; Stoddart, J. F. *Acc. Chem. Res.* **2005**, *38*, 1. (c) Brage, D. *Chem. Commun.* **2003**, 2751. (d) Seidel, S. R.; Stang, P. J. *Acc. Chem. Res.* **2002**, *35*, 972. (e) Fujita, M.; Umemoto, K.; Yoshizawa, M.; Fujita, N.; Kusukawa, T.; Biradha, K. *Chem. Commun.* 2001, 509. (f) Férey, G.; Mellot-Draznieks, C.; Serre, C.; Millange, F. *Acc. Chem. Res.* **2005**, *38*, 217.

(2) (a) Reger, D. L.; Wright, T. D.; Semeniuc, R. F.; Grattan, T. C.; Smith, M. D. *Inorg. Chem.* **2001**, *40*, 6212. (b) Zaman, M. B.; Smith, M. D.; Zurloye, H. C. *Chem. Commun*. **2001**, 2256. (c) Kitaura, R.; Seki, K.; Akiyama, G.; Kitagawa, S. *Angew. Chem., Int. Ed.* **2003**, *42*, 428. (d) Kitaura, R.; Fujimoto, K.; Noro, S.; Kondo, M.; Kitagawa, S. *Angew. Chem., Int. Ed*. **2002**, *41*, 133. (e) Bu, X. H.; Chen, W.; Lu, S. L.; Zhang, R. H.; Liao, D. Z.; Bu, W. M.; Shionoya, M.; Brisse, F.; Ribas, J. *Angew. Chem., Int. Ed.* **2001**, *40*, 3201. (f) Moulton, B.; Zaworotko, M. J. *Chem. Rev.* **2001**, *101*, 1629. (g) Gutschke, S. O. H.; Price, D. J.; Powell, A. K.; Wood, P. T. *Angew. Chem., Int. Ed.* **2001**, *40*, 1920. (h) Stupp, S. I.; Braun, P. V. *Science* **1997**, *277*, 1242. (i) Finn, R. C.; Zubieta, J. *J. Phys. Chem. Solids* **2001**, *62*, 1513. (j) Finn, R. C.; Lam, R.; Greedan, J. E.; Zubieta, J. *Inorg. Chem.* **2001**, *40*, 3745.

(3) (a) Wan, B. Z.; Anthony, R. G.; Peng, G. Z.; Clearfield, A. *J. Catal.* **1994**, *101*, 19. (b) Katz, H. E. *Chem. Mater.* **1994**, *6*, 2227. (c) Thompson, M. E. *Chem. Mater.* **1994**, *6*, 1168. (d) Deniaud, D.; Schöllhorn, B.; Mansuy, D.; Rouxel, J.; Battioni, P.; Bujoli, B. *Chem. Mater.* **1995**, *7*, 995. (e) Brousseau, L. C.; Aurentz, D. J.; Benesi, A. J.; Mallouk, T. E. *Anal. Chem.* **1997**, *69*, 688. (f) Bujoli, B.; Lane, S. M.; Nonglaton, G.; Pipelier, M.; Léger, J.; Talham, D. R.; Tellier, C. *Chem.*—*Eur. J.* **2005**, *11*, 1980.

(4) (a) Hix, G. B.; Kariuki, B. M.; Kitchin, S.; Tremayne M. *Inorg. Chem.* **2001**, *40*, 1477. (b) Cabeza, A.; Aranda, M. A. G.; Bruque, S.; Poojary, M. D.; Clearfield, A.; Sanz, J. *Inorg. Chem.* **1998**, *37*, 4168. (c) Fredoueil, F.; Penicaud, V.; Bujoli-Doeuff, M.; Bujoli, B. *Inorg. Chem.* **1997**, *36*, 4702.

10.1021/ic052095h CCC: $33.50

Chart 1. Coordination Modes of APD

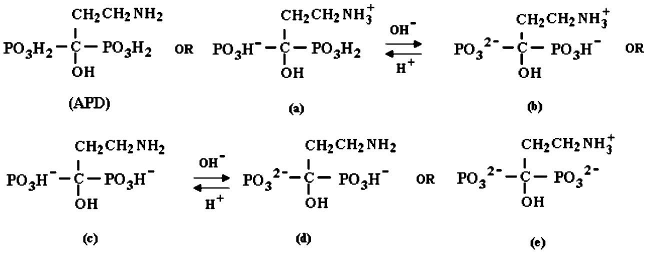

pillars between the inorganic layers, and it is well documented that the interlayer space can be adjusted by changing the length of organic chain (*n*) between two phosphonic acid groups.[5] If a fixed length of organic chain (*n*) and an organic pedant are introduced into the framework of diphosphonic acid, what will happen?

Organic amines, as good H-bond donors, are usually used as structure-directing agents in the syntheses of metal organodiphosphonates.[6] In the present work, an organic group containing a nitrogen atom is introduced as a pendant into the framework of an organodiphosphonic acid. As shown in Chart 1, pamidronate (3-ammonium-1-hydroxypropylidene-1,1-bisphosphonate, APD) possesses a hydrophilic organic pendant $NH_2CH_2CH_2-$, which is a potent inhibitor of osteoclast-mediated bone resorption and is indicated for hypercalcemia, osteolytic metastases, and Paget's disease of the bone.[7] Novel roles of APD in other diseases have also been suggested.[8] Additional fields where APD has found useful applications include bone imaging[9a] and organometallic chemistry.[9b] Because of the importance of APD, there has been increased interest in elucidating the coordination chemistry of APD. The investigation of the versatility of its coordination toward divalent metals would be helpful in understanding the adsorption of the drug onto bone, in which the coordination to calcium is involved. However, the crystal structures of metal−APD complexes have rarely been reported in previous work.[10] Because of the coexistence of one amino group and two phosphonate groups in APD, APD is expected to behave like an amino acid and exhibit zwitterionic (cationic and anionic) properties at weak acidic conditions.

In the present work, we hydrothermally synthesized five novel metal−APD complexes under similar conditions. Their structures span zero, one, two, and three dimensions, on the basis of the different binuclear secondary building units (SBUs) and different coordination modes of APD. The intramolecular (or intermolecular) H-bonds between the organic pendant of APD and phosphonate groups (or water) in their structures have been discussed. Compounds **1**−**5** exhibit different photoluminescence properties.

Experimental Section

General Considerations. All chemicals purchased were reagent grade and were used without further purification. C, H, N elemental analyses were performed on a Perkin-Elmer 240c elemental analyzer. Infrared spectra were recorded as KBr pellets on a Nicolet 170SXFT/IR spectrometer. Excitation and emission spectra were obtained on a RF-5301PC spectrofluorometer equipped with a 450 W xenon lamp as the excitation source. All measurements were performed at room temperature.

APD. APD was prepared according to the literature method.[11] Elemental Anal. Calcd for $C_3H_{11}NP_2O_7$: C, 15.32; H, 4.68; N, 5.96. Found: C, 15.51; H, 4.80; N, 5.88. IR (cm^{-1}): 3153(s), 1634(m), 1549(s), 1399(w), 1232(w), 1175(s), 1130(s), 1085(s), 995(s), 940(s), 827(m), 681(w), 490(m).

$Ni_2(C_3NH_{10}P_2O_7)_4 \cdot 4H_2O$ (1). A mixture of $Ni(NO_3)_2 \cdot 6H_2O$ (0.5 mmol, 0.145 g), APD (0.5 mmol, 0.118 g), and water (10 mL) was sealed in a Teflon-lined autoclave and heated at 160 °C for 3 days, followed by slow cooling to room temperature. The resulting green needlelike crystals of **1** were isolated by mechanical separation from a green amorphous solid, and then they were washed with water (yield = ca. 50% based on Ni). Elemental Anal. Calcd for $C_{12}H_{48}Ni_2N_4P_8O_{32}$: C, 12.79; H, 4.26; N, 4.97. Found: C, 12.67; H, 4.40; N, 4.98. IR (cm^{-1}): 3174(s), 1632(m), 1489(m), 1410(w), 1331(w), 1136(s), 1074(s), 1023(s), 982(s), 918(s), 782(w), 685(m).

$Co(C_3NH_9P_2O_7) \cdot H_2O$ (2). A mixture of $Co(NO_3)_2 \cdot 6H_2O$ (0.5 mmol, 0.146 g), APD (0.5 mmol, 0.118 g), and water (10 mL) was adjusted to pH 2.8 with a by 2 N NaOH aqueous solution; it was sealed in a Teflon-lined autoclave, heated at 160 °C for 3 days, and then slowly cooled to room temperature. The resulting red column crystals of **2** were filtered off and washed with water (yield = ca. 60% based on Co). Elemental Anal. Calcd for $C_3H_{11}CoNP_2O_8$: C, 11.61; H, 3.55; N, 4.52. Found: C, 11.69; H, 3.45;

---

(5) (a) Soghomonian, V.; Chen, Q.; Haushalter, R. C.; Zubieta, J. *Angew. Chem., Int. Ed. Engl.* **1995**, *34*, 223. (b) Poojary, D. M.; Zhang, B.; Bellinghausen, P.; Clearfield, A. *Inorg. Chem.* **1996**, *35*, 5254. (c) Bonavia, G.; Haushalter, R. C.; O'Connor, C. J.; Zubieta, J. *Inorg. Chem.* **1996**, *35*, 5603. (d) Alberti, G.; Vivani, R.; Marmottini, F.; Zappelli, P. *J. Porous Mater.* **1998**, *5*, 205. (e) Petruska, M. A.; Talham, D. R. *Chem. Mater.* **1998**, *10*, 3672. (f) Clearfield, A. *Chem. Mater.* **1998**, *10*, 2801. (g) Distler, A.; Lohse, D. L.; Sevov, S. C. *Dalton Trans.* **1999**, 1805. (h) Alberti, G.; Brunet, E.; Dionigi, C.; Juanes, O.; de la Mata, M. J.; Rodriguez-Ubis, J. C.; Vivani, R. *Angew. Chem., Int. Ed.* **1999**, *38*, 3351. (i) Zheng, L.; Song, H.; Lin, C.; Wang, S.; Hu, Z.; Yu, Z.; Xin, X. *Inorg. Chem.* **1999**, *38*, 4618. (j) Zheng, L.; Song, H.; Duan, C.; Xin, X. *Inorg. Chem.* **1999**, *38*, 5061. (k) Serre, C.; Férey, G. *Inorg. Chem.* **1999**, *38*, 5370. (l) Cao, G.; Guillou, N.; Nogues, M.; Cheetham, A. K.; Férey, G. *Chem. Mater.* **1999**, *11*, 2937. (m) Neff, G. A.; Helfrich, M. R.; Clifton, M. C.; Page, C. J. *Chem. Mater.* **2000**, *12*, 2363. (n) Riou, D.; Belier, F.; Serre, C.; Nogues, M.; Vichard, D.; Férey, G. *Int. J. Inorg. Mater.* **2000**, *2*, 29. (o) Altomare, A.; Bellitto, C.; Ibrahim, S. A.; Mahmoud, M. R.; Rizzi, R. *Dalton Trans.* **2000**, 3913.

(6) (a) Yin, P.; Zheng, L. M.; Gao S.; Xin X. Q. *Chem. Commun.* **2001**, 2346. (b) Finn, R. C.; Zubieta, J. *Dalton Trans.* **2000**, 1821. (c) Finn, R. C.; Zubieta, J. *Inorg. Chim. Acta* **2002**, *335*, 131. (d) Finn, R. C.; Zubieta J. *Inorg. Chim. Acta* **2002**, 332, 191. (e) Yin, P.; Gao, S.; Zheng, L. M.; Xin, X. Q. *Chem. Mater.* **2003**, *15*, 3233. (f) Zheng, L. M.; Gao, S.; Yin, P.; Xin, X. Q. *Inorg. Chem.* **2004**, *43*, 2151. (g) Song, H. H.; Yin, P.; Zheng, L. M.; Korp, J. D.; Jacobson, A. J.; Xin, X. Q. *Dalton Trans.* **2002**, 2752. (h) Song, H. H.; Zheng, L. M.; Wang, Z.; Yan, C.-H.; Xin, X.-Q. *Inorg. Chem.* **2001**, *40*, 5024.

(7) Widler, L.; Jaeggi, K. A.; Glatt, M.; Muller, K.; Bachmann, R.; Bisping, M.; Born, A. R.; Cortesi, R.; Guiglia, G.; Jeker, H.; Klein, R.; Ramseier, U.; Schmid, J.; Schreiber, G.; Seltenmeyer, Y.; Green, J. R. *J. Med. Chem.* **2002**, *45*, 3721.

(8) (a) Wolf, J. S.; Stoller, M. L. *J. Urol.* **1994**, *152*, 1609. (b) Dunn, C. J.; Slatter, J. G.; Nugent, R. A. *Drugs*, **1998**, *1*, 429. (c) Reid, I. R. *Curr. Opin. Rheumatol.* **2003**, *15*, 458.

(9) (a) Love, C.; Din, A. S.; Tomas, M. B.; Kalapparambath, T. P.; Palestro, C. J. *RadioGraphics* **2003**, *23*, 341. (b) Stock, N.; Bein, T. *J. Solid State Chem.* **2002**, *167*, 330.

(10) (a) Vega, D.; Fernandez, D.; Ellena, J. A. *Acta Crystallogr.* **2002**, *C58*, m77. (b)Fernandez, D.; Vega, D.; Goeta, A. *Acta Crystallogr.* **2002**, *C58*, m494. (c) Fernandez, D.; Polla, G.; Vega, D.; Ellena, J. A. *Acta Crystallogr.* **2004**, *C60*, m73.

(11) (a) Ernest, M.; Mujahid, S.; John, T. S. *J. Labelled Compd. Radiopharm.* **1982**, *19*, 1145. (b) Liang, G. L.; Hu, M. Y.; Wang, B. C. *J. Chin. Modern Appl. Med.* **1999**, *16*, 37.

Table 1. Crystal Data and Structure Refinements for Compounds **1**−**5**

	1	**2**	**3**	**4**	**5**
formula	$C_{12}H_{48}Ni_2N_4P_8O_{32}$	$C_3H_{11}CoNP_2O_8$	$C_3H_{11}MnNP_2O_8$	$C_3H_{11}ZnNP_2O_8$	$C_6H_{20}Cu_3N_2P_4O_{16}$
M	1121.69	310.00	306.01	314.42	690.74
cryst syst	monoclinic	triclinic	triclinic	monoclinic	monoclinic
space group	$P2_1/c$	$P\bar{1}$	$P\bar{1}$	$P2_1/c$	$P2_1/c$
a (Å)	12.120(4)	5.4483(19)	5.570(11)	9.2565(13)	10.232(4)
b (Å)	12.481(4)	8.828(3)	8.883(18)	10.2110(14)	7.961(3)
c (Å)	12.419(4)	9.809(4)	9.84(2)	10.1356(14)	11.016(4)
α (deg)	90	91.748(5)	92.03(3)	90	90
β (deg)	104.804(4)	103.976(5)	104.30(3)	104.530(2)	101.448(5)
γ (deg)	90	97.928(5)	97.45(3)	90	90
V (Å^3)	1816.3(9)	452.5(3)	466.5(16)	927.4(2)	879.5(6)
Z	2	2	2	4	2
ρ_{calcd} (g cm^{-3})	2.051	2.275	2.179	2.252	2.608
μ (mm^{-1})	1.509	2.277	1.784	3.019	4.053
F(000)	1152	314	310	632	690
GOF on F^2	1.058	1.089	1.106	1.049	1.078
final R^a indices	$R_1 = 0.0393$	$R_1 = 0.0417$	$R_1 = 0.0535$	$R_1 = 0.0274$	$R_1 = 0.0237$
$[I > 2\sigma(I)]$	$R_2 = 0.0909$	$R_2 = 0.1088$	$R_2 = 0.1094$	$R_2 = 0.0706$	$R_2 = 0.0603$

[a] $R_1=\sum||F_o| - |F_c||/\sum|F_o|$; $R_2=\sum[w(F_o^2 - F_c^2)^2]/\sum[w(F_o^2)^2]^{1/2}$.

N, 4.58. IR (cm^{-1}): 3441(m), 3282 (s), 2981(m), 1618(m), 1491(m), 1410(w), 1320(w), 1151(s), 1108(s), 1062(s), 983 (m), 918(m), 782(w), 579(m).

$Mn(C_3NH_9P_2O_7)\cdot H_2O$ (3). The synthesis of **3** was similar to that of **2** except that $Mn(NO_3)_2\cdot 6H_2O$ (0.5 mmol, 0.144 g)was used instead of $Co(NO_3)_2\cdot 6H_2O$. The pink column crystals of **3** were filtered off and washed with water (yield = ca. 60% based on Mn). Elemental Anal. Calcd for $C_3H_{11}MnNP_2O_8$: C, 11.76; H, 3.59; N, 4.58. Found: C, 11.68; H, 3.61; N, 4.62. IR (cm^{-1}): 3441(m), 3282 (s), 2981(m), 1618(m), 1491(m), 1410(w), 1320(w), 1151(s), 1108(s), 1062(s), 983 (m), 918(m), 782(w), 579(m).

$Zn(C_3NH_9P_2O_7)\cdot H_2O$ (4). The synthesis of **4** was similar to that of **2** except that $Zn(NO_3)_2$ (0.5 mmol, 0.149 g) was used instead of $Co(NO_3)_2\cdot 6H_2O$ and the mixture was adjusted to pH 3.6 with a 2 N NaOH aqueous solution. The resulting colorless platelike crystals of **4** were isolated by mechanical separation from a white amorphous solid, and then they were washed with water (yield = ca. 70% based on Zn). Elemental Anal. Calcd. for $C_3H_{11}ZnNP_2O_8$: C, 11.39; H, 3.48; N, 4.43. Found: C, 11.49; H, 3.45; N, 4.48. IR (cm^{-1}): 3477(s), 2920(s), 1623(m), 1541(m), 1478(w), 1354(w), 1115(s), 1085(s), 983 (m), 782(w), 685(m).

$Cu_3(C_3NH_8P_2O_7)_2\cdot 2H_2O$ (5). The synthesis of **5** was similar to that of **2** except that $Cu(NO_3)_2$ (0.5 mmol, 0.121 g) was used instead of $Co(NO_3)_2\cdot 6H_2O$ and the mixture was adjusted to pH 4.2 with a 2 N NaOH aqueous solution. The resulting blue block crystals of **5** were filtered off and washed with water (yield = ca. 85% based on Cu). Elemental Anal. Calcd for $C_6H_{20}Cu_3N_2P_4O_{16}$: C, 10.40; H, 2.89; N, 4.05. Found: C, 10.49; H, 2.75; N, 4.08. IR (cm^{-1}): 3568(s), 3486(m), 3207(s), 3059(s), 1657(m), 1468(m), 1377(w), 1122(s), 1074(s), 918 (s), 850(m), 680 (m), 570 (s)

Crystallographic Studies. XRD data of compounds **1**−**5** were collected on a Bruker-AXS CCD area detector-equipped diffractometer with graphite-monochromatized Mo Kα ($\lambda = 0.71073$ Å) radiation at room temperature. A total of 9377 (3200 unique, $R_{int} = 0.0367$) reflections of compound **1** ($-11 \le h \le 14$, $-14 \le k \le 12$, $-14 \le l \le 14$, $2.35 < \theta < 25.01$), a total of 2411 (1587 unique, $R_{int} = 0.0285$) reflections of **2** ($-6 \le h \le 6$, $-7 \le k \le 10$, $-11 \le l \le 10$, $2.14 < \theta < 25.01$), a total of 2383 (1610 unique, $R_{int} = 0.0337$) reflections of **3** ($-6 \le h \le 6$, $-9 \le k \le 10$, $-11 \le l \le 10$, $2.14 < \theta < 25.00$), a total of 5895 (2246 unique, $R_{int} = 0.0301$) reflections of **4** ($-12 \le h \le 7$, $-12 \le k \le 13$, $-13 \le l \le 13$, $2.27 < \theta < 28.30$), and a total of 4459 (1546 unique, $R_{int} = 0.0278$) reflections of **5** ($-11 \le h \le 12$, $-9 \le k \le 8$, $-12 \le l \le 13$, $2.48 < \theta < 25.01$) were measured. An empirical absorption correction from the ψ scan was applied. All the structures were solved by direct methods and expanded using Fourier techniques. The non-hydrogen atoms were refined anisotropically. Hydrogen atoms attached to hydroxyl group and phosphonate groups of APD were located in the Fourier difference maps. All of the other hydrogen atoms were placed in calculated positions. All calculations were performed using the SHELXTL97 program.[12] The CCDC reference numbers are the following: 286870 for compound **1**, 286868 for compound **2**, 286867 for compound **3**, 286871 for compound **4**, 286869 for compound **5**. Crystal data and structure refinements for compounds **1**−**5** are listed in Table 1. Selected bond lengths and angles for compounds **1**−**5** are listed in Tables 2 and 4−6. Selected H-bonds in compounds **1**−**5** are listed in Table 3. Further details are provided in the Supporting Information.

Table 2. Selected Bond Lengths (Å) and Angles (deg) for Compound **1**[a]

Ni(1)−O(15)	2.076(3)	Ni(1)−O(4)	2.050(3)
Ni(1)−O(1)	2.076(3)	Ni(1)−O(9)#1	2.073(3)
Ni(1)−O(11)#1	2.037(3)	Ni(1)−O(8)	2.044(3)
O(8)−Ni(1)−O(15)	83.25(14)	O(4)−Ni(1)−O(15)	89.59(14)
O(8)−Ni(1)−O(1)	176.78(12)	O(9)#1−Ni(1)−O(15)	173.81(13)
P(1)−C(1)−P(3)	112.9(2)	P(4)−C(4)−P(2)	110.8(3)

[a] Symmetry transformations used to generate equivalent atoms: #1 $-x + 2$, $-y + 2$, $-z + 1$.

Results and Discussion

Synthesis. The preparations of compounds **1**−**5** rely on well-established hydrothermal methods. Under such conditions, the different solubilities of the organic and inorganic starting materials are alleviated. The hydrothermal temperature (below 200 °C) avoids decomposition of the organic components and promotes "self-assembly" of crystalline metastable phases from simple molecular precursors.

In the present work, the preparations of compounds **1**−**5** were not susceptible to the reaction temperature and reaction time. In general, solutions of APD and metal salt were treated

---

(12) (a) Sheldrick, G. M. *SHELXS97, Program for Crystal Structure Solution*; University of Göttingen: Göttingen, Germany, 1997. (b) Sheldrick, G. M. *SHELXL97, Program for Crystal Structure Refinement*; University of Göttingen: Göttingen, Germany, 1997.

Table 3. Distances (Å) and Angles (deg) Involving Selected H-bonds for Compounds **1**−**5**

A	H	B	A···B	H···A	∠B−H···A
			1		
O(3)	H(1A)	N(1)	2.904	2.135	144.1
O(1)	H(1C)	N(1)	3.224	2.377	159.0
O(16)	H(1B)	N(1)	2.856	1.984	166.1
O(2)	H(2A)	N(2)	2.948	2.089	161.8
O(8)	H(2B)	N(2)	2.840	2.010	154.5
O(16)	H(2C)	N(2)	2.947	2.092	160.7
			2		
O(8)	H(1B)	N(1)	3.127	2.502	130.2
O(2)	H(1B)	N(1)	3.023	2.362	133.9
O(4)	H(1A)	N(1)	3.096	2.458	131.5
O(5)	H(1A)	N(1)	2.863	2.139	141.6
			3		
O(8)	H(1B)	N(1)	3.196	2.707	115.8
O(5)	H(1B)	N(1)	2.820	2.015	149.9
O(4)	H(1B)	N(1)	3.097	2.435	131.5
O(6)	H(1A)	N(1)	2.863	2.012	159.8
			4		
O(3)	H(1A)	N(1)	2.863	2.018	157.9
O(8)	H(1B)	N(1)	2.815	2.085	138.6
O(5)	H(1C)	N(1)	2.772	1.886	173.4
			5		
O(2)	H(1A)	N(1)	3.003	2.138	172.4
O(3)	H(1B)	N(1)	2.962	2.049	163.4
O(5)	H(1C)	N(1)	2.782	2.549	136.3
O(6)	H(1C)	N(1)	2.788	1.991	145.7

hydrothermally for 3−5 days at temperatures of 150−180 °C to produce crystalline products in moderate yields (50−85%). The syntheses were largely dependent on the molar ratio of reactants, and the 1:1 molar ratio of APD/metal ion represented the optimized condition for the preparation of compounds **1**−**5**. It is noteworthy that the reactions were not very susceptible to the species of counteranions in metal sources. Substitution of $M(NO_3)_2$ (M = Ni, Co, Mn, Zn, Cu) with MCl_2 also resulted in the desired products. However, the reaction pH values played very important roles in the crystallization of compounds **1**−**5.** The initial pH values of the mixtures for the preparations of compounds **1**−**5** were 1.7, 2.8, 2.8, 3.6, and 4.2, respectively. Minor variations in the pH values of the reaction solutions result in microcrystalline or amorphous materials. This is probably the result of the coexistence of one amino group and two phosphonate groups in the APD molecule. At weak acidic conditions, these groups can be protonated or deprotonated (Chart 1**),** and this makes APD behave like an amino acid and exhibit zwitterionic (cationic and anionic) properties. At different pH values, the degree of protonation or deprotonation are different, and different intramolecular H-bonds can be formed between the amino group and the phosphonate groups (Table 3); thus APD can exhibit different affinities for water molecules (Table 3) and metal ions.

Crystal Structure of $Ni_2(C_3NH_{10}P_2O_7)_4{\cdot}4H_2O$ (1). A molecular binuclear nickel cluster (Ni···Ni = 5.084 Å) is observed in compound **1**, which consists of four APD, and the asymmetric unit of compound **1** contains one Ni(II), two APD, one coordinated water, and one dissociated water. The oxygen atom of the dissociated water has two positions, O(16) and O(16′), because of crystallographic disorder; their occupancy factors are 80 and 20%, respectively. One phosphorus atom of APD has three positions, P (4), P(4′), and P(4″),because of crystallographic disorder; their occupancy factors are 70, 15, and 15%, respectively. Ni(1) exhibits a distorted octahedral geometry and is six-coordinated by one oxygen atom from the aqua ligand and five oxygen atoms from the phosphonate groups of three APD. As shown in Figure 1a, O(15) is from water [Ni−O = 2.076(3) Å]; O(1) and O(4) are from two phosphonate groups of one APD [Ni−O = 2.050(3)−2.076(3) Å]. O(9A) and O(11A) are from two phosphonate groups of another APD [Ni−O = 2.037(3)−2.073(3) Å], and O(8) is from the third APD [Ni−O = 2.044(3) Å]. O(9) and O(11), which are from the third APD, are bonded to Ni(1A). Thus, the binuclear Ni(II) cluster is linked by two symmetrical APD molecules (Figure 1). Another two APD molecules in the cluster have not participated in bridging the two Ni(II) centers; they are bonded to Ni(1) and Ni(1A), respectively. The two coordination modes of APD are shown in Scheme 1a and b. The hydroxyl groups of the four ADP are uncoordinated. All the amino groups have been protonated, and they can form H-bonds with phosphonate groups or water molecules (Table 3).

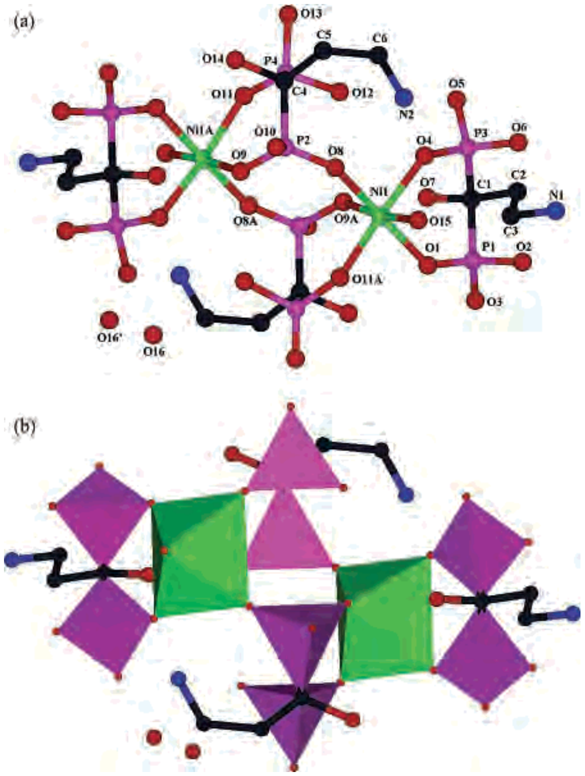

Figure 1. Ball and stick representation of $Ni_2(C_3NH_{10}P_2O_7)_4{\cdot}4H_2O$ **(1)**. Atoms with additional label A refer to the following symmetry operation: $-x + 2, -y + 2, -z + 1$ (H atoms omitted for clarity) (a). Polyhedral representation. $\{NiO_6\}$ octahedron is green, and the $\{PO_3C\}$ tetrahedron is pink (b).

Crystal Structure of $Co(C_3NH_9P_2O_7){\cdot}H_2O$ (2) and $Mn(C_3NH_9P_2O_7){\cdot}H_2O$ (3). Compounds **2** and **3** are isostructural. Therefore, we will restrict our description to the cobalt compound, **2**, and only mention pertinent points for the manganese compound, **3**, where appropriate.

In compound **2**, there is one crystallographically unique Co(II), one unique APD, and one unique dissociated water.

Scheme 1. Protonation or Deprotonation of APD in Compounds **1**−**5** in Weak Acidic Conditions

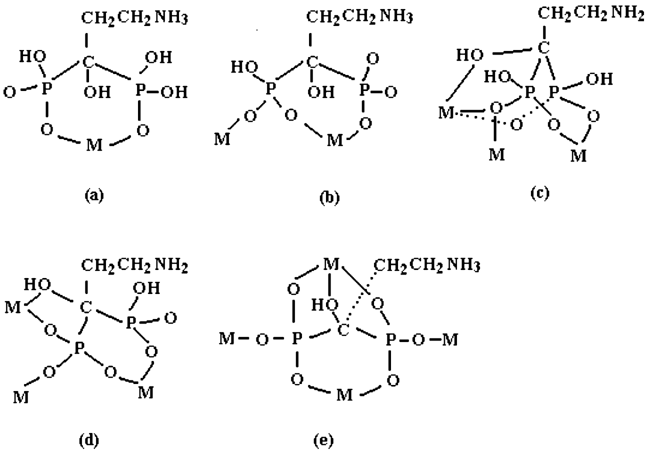

Co(1) exhibits an octahedral coordination sphere and is coordinated by six oxygen atoms from three APD (Figure 2). O(7), O(1), and O(4) are from the hydroxyl group and two phosphonate groups of one APD, respectively; O(4A) is from phosphonate group of another APD, and O(3C) and O(5C) are from two phosphonate groups of the third APD. The Co−O distances are in the range of 2.024(3)−2.284(3) Å, and the bond angles of O−Co−O range from 80.39(12) to 173.75(11)°. In compound **3**, the bond lengths of Mn−O range from 2.106(5) to 2.365(6) Å, and the bond angles of O−Mn−O are in the range of 75.64(16)−171.13(15)° (Table 4). APD ligands in compound **2** exhibit a uniform coordination mode (Scheme 1c): each phosphonate group has three oxygen atoms, and only one of them is uncoordinated; the two coordinated oxygen atoms are ligated to different Co(II) centers, and compound **2** exhibits a one-dimensional structure (Figure 2). Furthermore, among the four coordinated phosphonate oxygen atoms in one ADP, there is one oxygen atom, such as O(4A) which is μ_2-O, which connects two Co(II) centers. Thus Co(II) dimer (Co···Co = 3.225 Å) is observed in the one-dimensional framework (Mn···Mn in compound **3** is 3.359 Å). In other words, compound **2** exhibits a ladderlike structure, in which the rack is made up of the Co(II) dimer and each ladder is made up of two vertex-shared {PO_3C} tetrahedra (Figure 3). The amino groups of APD dangle out of the ladder (Figure 2) and form H-bonds with water molecules to generate a three-dimensional supramolecular network (Figure 4 and Table 3).

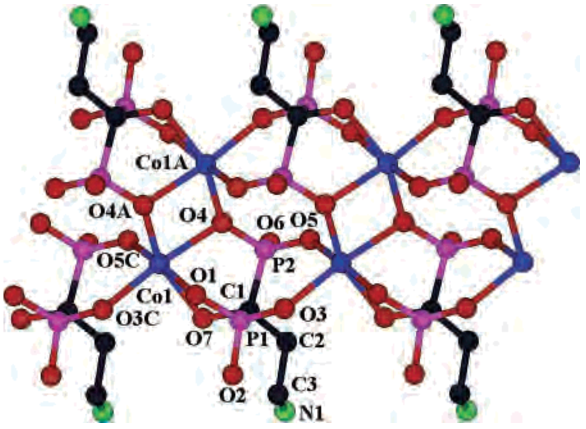

Figure 2. Ball and stick representation of Co($C_3NH_9P_2O_7$)·H_2O (**2**) (H atoms omitted for clarity). Atoms with additional labels A and C refer to the following symmetry operations: A −*x*, −*y* + 2, −*z*; C *x* − 1, *y*, *z*.

Table 4. Selected Bond Lengths (Å) and Angles (deg) for Compounds **2** and **3**[a]

	2		
Co(1)−O(1)	2.100(3)	Co(1)−O(4)	2.170(3)
Co(1)−O(7)	2.284(3)	Co(1)−O(4)#2	2.051(3)
Co(1)−O(5)#1	2.024(3)	Co(1)−O(3)#1	2.142(3)
O(3)#1−Co(1)−O(4)	173.75(11)	O(4)#2−Co(1)−O(4)	80.39(12)
P(1)−O(3)−Co(1)#3	132.16(18)	P(1)−C(1)−P(2)	110.0(2)
	3		
Mn(1)−O(6)#1	2.106(5)	Mn(1)−O(4)#2	2.106(5)
Mn(1)−O(2)#1	2.188(5)	Mn(1)−O(1)	2.203(5)
Mn(1)−O(4)	2.257(5)	Mn(1)−O(7)	2.365(6)
O(1)−Mn(1)−O(7)	75.64(16)	O(2)#1−Mn(1)−O(4)	171.13(15)
P(1)−C(1)−P(2)	111.5(3)	P(1)−O(2)−Mn(1)#3	131.5(2)

[a] Symmetry transformations used to generate equivalent atoms: #1 *x* − 1, *y*, *z*; #2 −*x*, −*y* + 2, −*z*; #3 *x* + 1, *y*, *z*.

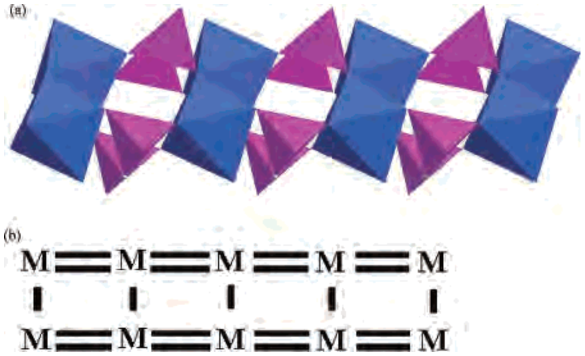

Figure 3. One-dimensional ladderlike structure of compound **2** (organic pendant $NH_2CH_2CH_2$− of APD and H atoms omitted for clarity). Polyhedral representation. {CoO_6} octahedron is blue, and the {PO_3C} tetrahedron is pink (a). Schematic illustration (b).

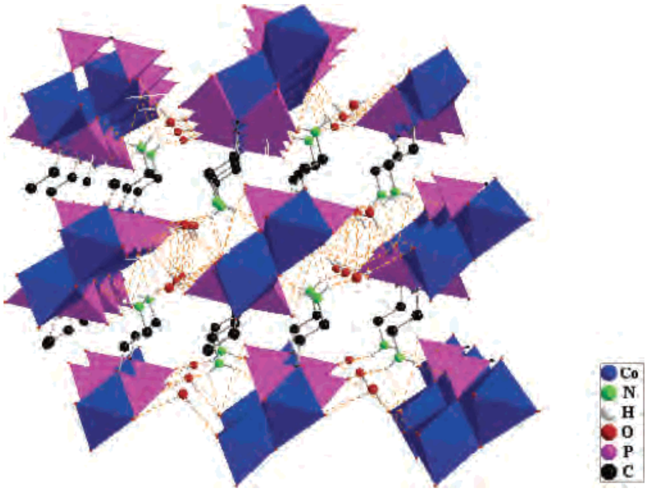

Figure 4. Crystal packing of compound **2** viewed down the *a* axis (H atoms of methylene groups omitted for clarity).

Crystal Structure of Zn($C_3NH_9P_2O_7$)·H_2O (4) Similar to compounds **2** and **3**, the asymmetric unit of compound **4** contains one Zn(II), one APD, and one dissociated water. However, compound **4** exhibits a distinctly different framework from those of compounds **2** and **3**. In compound **4**, Zn(1) exhibits a distorted trigonal bipyramidal geometry and

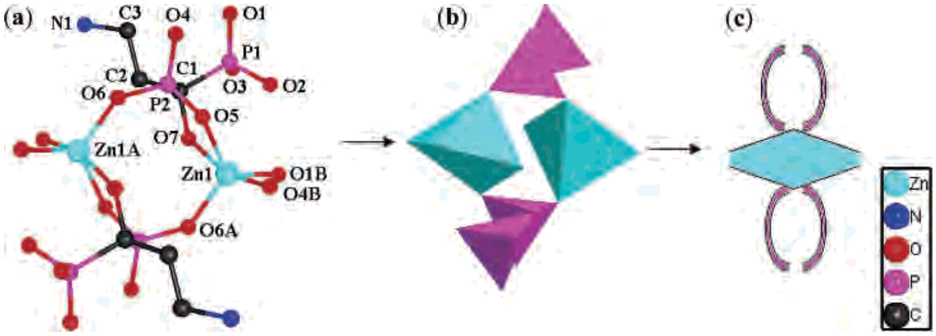

Figure 5. Ball and stick representation f $Zn(C_3NH_9P_2O_7)\cdot H_2O$ **(4)**. Atoms with additional labels A and B refer to the following symmetry operations: A −*x*, −*y*, −*z* + 1; B *x*, −*y* + 1/2, *z* + 1/2 (H atoms omitted for clarity) (a). Polyhedral representation (b) and schematic illustration (c) of the Zn(II) dimer (organic pendant $NH_2CH_2CH_2-$ of APD and H atoms omitted for clarity). $\{ZnO_5\}$ trigonal bipyramid is sapphire, and the $\{PO_3C\}$ tetrahedron is pink.

Table 5. Selected Bond Lengths (Å) and Angles (deg) for Compound **4**[a]

Zn(1)−O(6)#1	1.9204(16)	Zn(1)−O(5)	1.9465(16)
Zn(1)−O(1)#2	1.9991(16)	Zn(1)−O(4)#2	2.0126(16)
Zn(1)−O(7)	2.4528(17)	O(1)−Zn(1)#3	1.9991(16)
O(5)−Zn(1)−O(7)	75.85(6)	O(4)#2−Zn(1)−O(7)	163.47(6)
O(6)#1−Zn(1)−O(5)	117.49(7)	O(1)#2−Zn(1)−O(4)#2	93.19(7)
P(1)−C(1)−P(2)	113.41(11)	C(1)−O(7)−Zn(1)	114.11(12)

[a] Symmetry transformations used to generate equivalent atoms: #1 −*x*, −*y*, −*z* + 1; #2 *x*, −*y* + 1/2, *z* + 1/2; #3 *x*, −*y* + 1/2, *z* − 1/2.

is coordinated by five oxygen atoms from three APD molecules. As shown in Figure 5a, O(1B) and O(4B) are from two phosphonate groups of one APD; O(5) and O(7) are from the phosphonate group and hydroxyl group of another APD, and O(6A) is from the phosphonate group of the third APD. The APD ligands in compound **3** also exhibit a uniform coordination mode; however, it is different from those in compounds **2** and **3**. As shown in scheme 1d, the two phosphonate groups of one APD molecule coordinate in a nonequivalent manner: one phosphonate group links three Zn(II) centers via its three oxygen atoms, while another phosphonate group is only bonded to one Zn(II), leaving two oxygen atoms uncoordinated. The Zn−O distances are in the range of 1.9204(16)−2.4528(17) Å, and the bond angles of O−Zn−O range from 75.85(6) to 163.47(6)° (Table 5). The Zn(II) dimer (Zn···Zn = 4.373 Å) is observed in the structure which is constructed by two APD molecules linking two Zn(II) centers (Figure 5a). If we take the Zn(II) dimer as a single node, this SBU becomes a four-connected node (Figure 5b and c). However, the four links only orient in two different directions, and each pair “chelates” to another SBU. The adjacent SBUs are cross-linked, and compound **2** exhibits a two-dimensional gridlike structure. There are two links between two SBUs, so the framework is very similar to a (4, 4) topological net with a double bond between two nodes (Figure 6). Each grid is composed of four $\{ZnO_5\}$ trigonal bipyramids and four pairs of $\{PO_3C\}$ tetrahedra, and the size of the grid is ca. 5.4 × 6.4 Å^2 in terms of the neighboring Zn···Zn distance. The organic pendant NH_2CH_2-CH_2- of APD is dangling into the interlayer region, and its protonated nitrogen atom forms H-bonds with phosphonate groups or dissociated water (Figure 7 and Table 3).

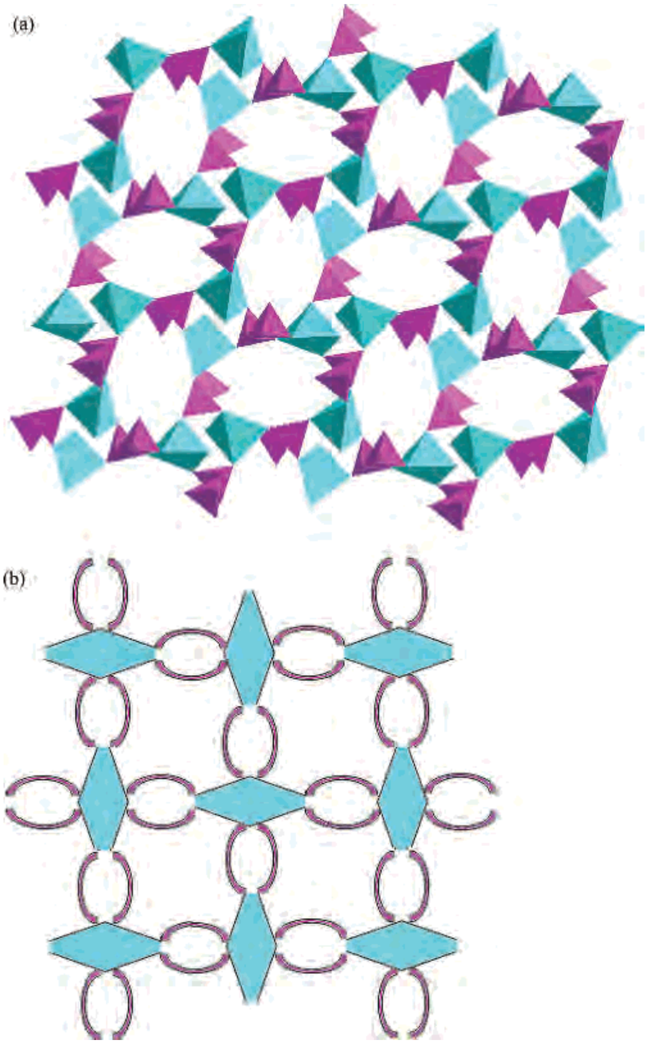

Figure 6. Two-dimensional gridlike structure of compound **4** (organic pendant $NH_2CH_2CH_2-$ of APD and H atoms omitted for clarity). Polyhedral representation (a) and schematic illustration (b).

Crystal Structure of $Cu_3(C_3NH_8P_2O_7)_2\cdot 2H_2O$ (5). The asymmetric unit of compound **5** contains two Cu(II), one APD, and one coordinated water. Cu(1) exhibits an octahedral coordination sphere and is coordinated by one oxygen atom from an aqua ligand and five oxygen atoms from three APD molecules (Figure 8). O(8) is from water; O(7), O(1), and O(4) are from the hydroxyl group and two phosphonate groups of one APD, respectively, and O(3A) and O(6B) are from the phosphonate groups of two APD. Cu(2) exhibits a square planar coordination sphere and is coordinated by four

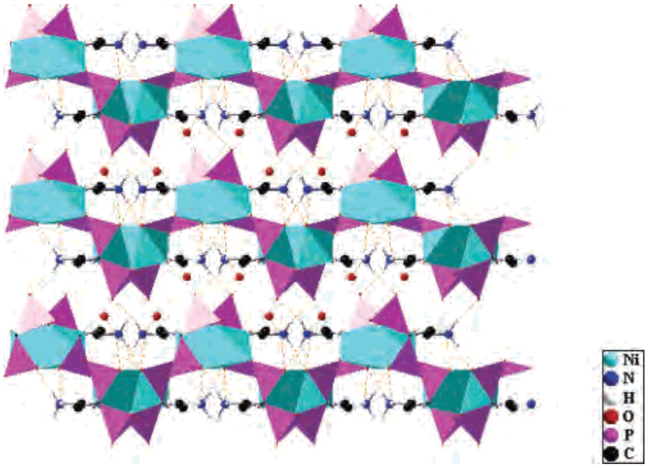

Figure 7. Crystal packing of compound **4** viewed down the *c* axis (H atoms of methylene groups omitted for clarity).

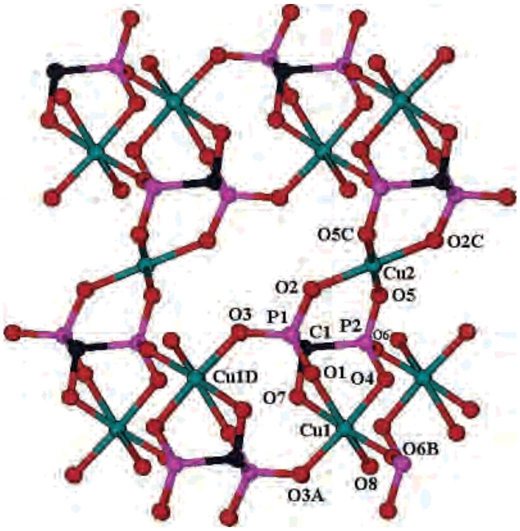

Figure 8. Ball and stick representation of $Cu_3(C_3NH_8P_2O_7)_2{\cdot}2H_2O$ (**5**); atoms with additional labels A, B, C, and D refer to te following symmetry operations: A $-x + 1, -y, -z$; B $-x + 3/2, y - 1/2, -z + 1/2$; C $-x + 2, -y, -z$; D $-x + 3/2, y + 1/2, -z + 1/2$ (organic pendant $NH_2CH_2CH_2-$ of APD and H atoms omitted for clarity).

Table 6. Selected Bond Lengths (Å) and Angles (deg) for Compound **5**[a]

Cu(1)−O(3)#1	1.954(2)	Cu(1)−O(4)	1.968(2)
Cu(1)−O(6)#2	1.975(2)	Cu(1)−O(7)	2.148(3)
Cu(1)−O(8)	2.357(3)	Cu(1)−O(1)	2.396(2)
Cu(2)−O(5)#3	1.910(2)	Cu(2)−O(5)	1.910(2)
Cu(2)−O(2)	1.977(2)	Cu(2)−O(2)#3	1.977(2)
O(7)−Cu(1)−O(1)	78.76(9)	O(3)#1−Cu(1)−O(4)	176.23(9)
O(6)#2−Cu(1)−O(7)	173.69(10)	O(4)−Cu(1)−O(8)	86.00(10)
O(5)#3−Cu(2)−O(2)	86.73(10)	O(2)−Cu(2)−O(2)#3	180.0(2)
O(5)−Cu(2)−O(2)	93.27(10)	O(5)#3−Cu(2)−O(5)	180.00(15)
P(2)−C(1)−P(1)	109.79(17)	P(2)−O(6)−Cu(1)#4	135.16(14)

[a] Symmetry transformations used to generate equivalent atoms: #1 $-x + 1, -y, -z$; #2 $-x + 3/2, y - 1/2, -z + 1/2$; #3 $-x + 2, -y, -z$; #4 $-x + 3/2, y + 1/2, -z + 1/2$.

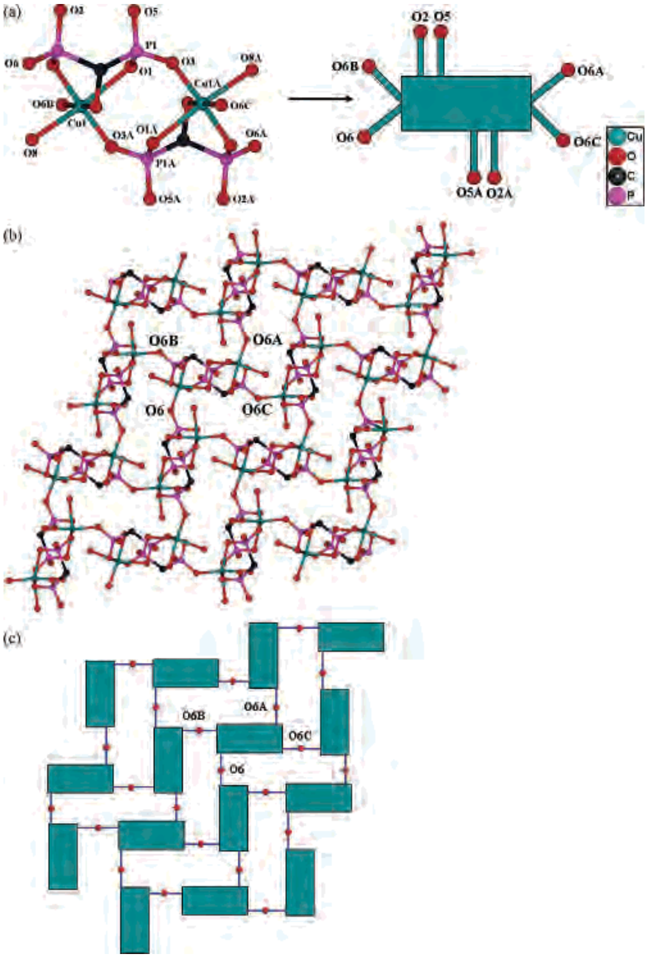

Figure 9. Eight-connected SBU in compound **5** (organic pendant NH_2-CH_2CH_2- of APD and H atoms omitted for clarity) (a). Two-dimensional layer with parquet motif in compound **5**. Ball and stick representation (b). Schematic illustration (**c**).

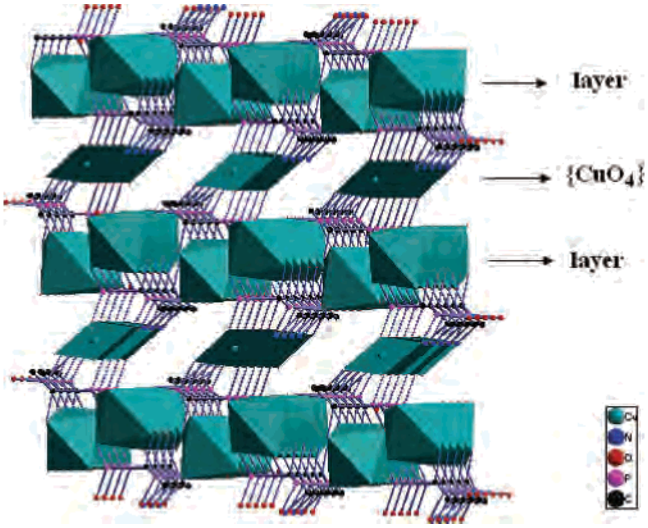

Figure 10. Two-dimensional layers pillared by $\{CuO_4\}$ planar squares to construct a three-dimensional architecture in compound **5**.

oxygen atoms from two APD. O(2) and O(5) are from two phosphonate groups of one APD; O(2C) and O(5C) are from two phosphonate groups of another APD. The Cu−O distances are in the range of 1.910(2)−2.396(2) Å, and the bond angles of O−Cu−O range from 78.76(9) to 180.0(2)° (Table 6). APD exhibits a uniform coordination fashion which is completely different from those in compounds **1**−**4**. As shown in Scheme 1e, all the oxygen atoms of APD, including those from hydroxyl group and two phosphonate groups, have been coordinated to the Cu(II) centers. APD acts as a heptadentate ligand, and each phosphonate group

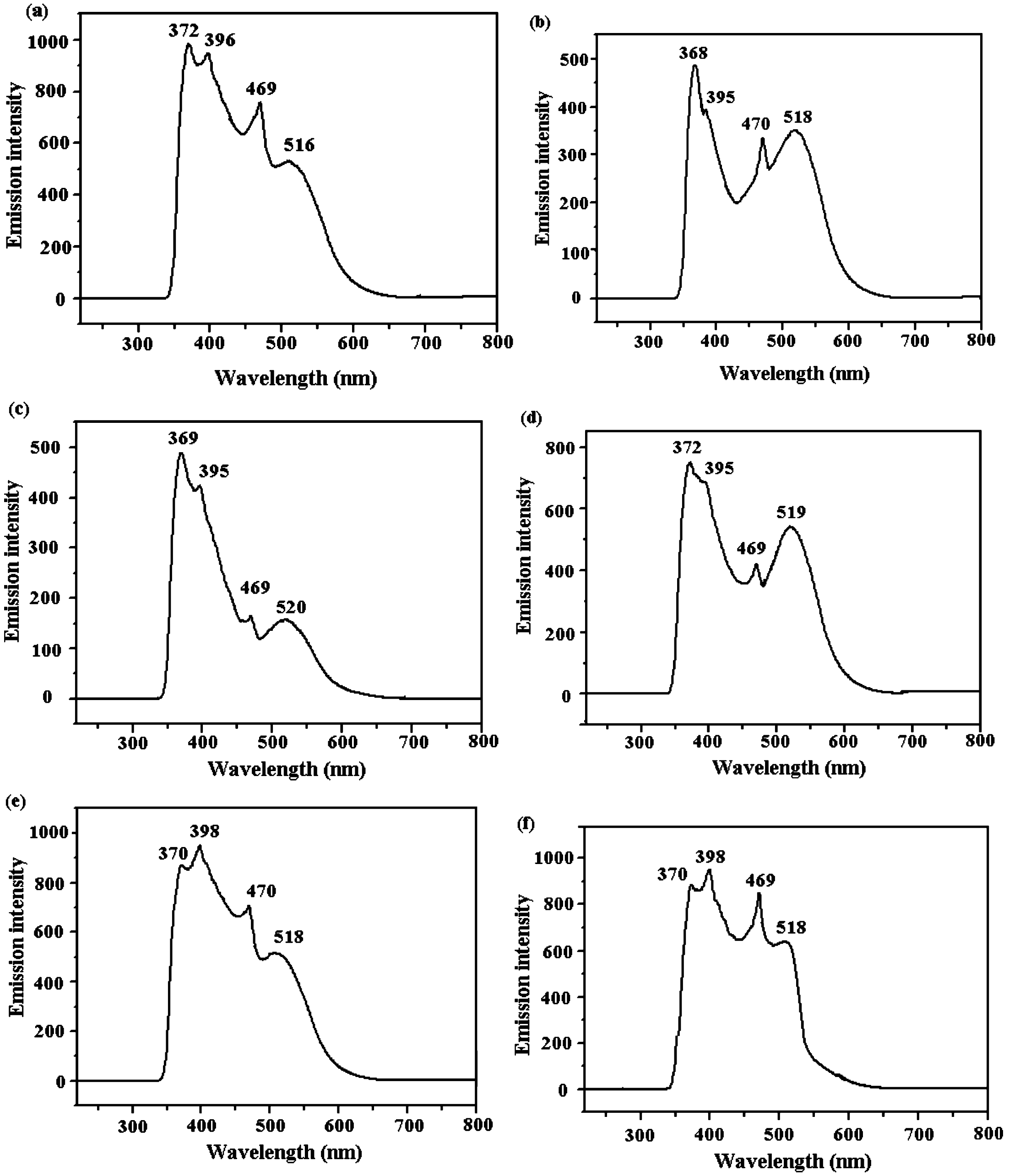

Figure 11. Solid-state emission spectra at room temperature of APD (a), compound **1** (b), compound **2** (c), compound **3** (d), compound **4** (e), and compound **5** (f).

links three Cu(II) centers via its three oxygen atoms. A dinuclear Cu(II) cluster (Cu···Cu = 4.839 Å) is observed in compound **5**; however, the metal dimer is different from those we mentioned above. As shown in Figure 9a, one SBU consists of two APD, and the two Cu(II) centers in the SBU are linked by two O−P−O bridges (O1−P1−O3 and O1A−P1A−O3A). If we take the SBU as a single node, it can be considered to be an eight-connected node (Figure 9a). One SBU is connected to four neighboring SBUs by four links. In other words, they are connected with each other by sharing four bridging-oxygen atoms, such as O(6), O(6B), O(6A), and O(6C); thus, a two-dimensional layer with a parquet motif is constructed (Figure 9b and c). Another four links in the SBU orient above and below the two-dimensional layer, and each pair chelates to the Cu(II) centers located in the interlayer region; thus, the two-dimensional layers with parquet motif were pillared by $\{CuO_4\}$ planar squares, and compound **5** exhibits an unusual three-dimensional architecture (Figure 8). The protonated amino groups of APD can form intramolecular H-bonds with phosphonate groups (Table 3).

IR Spectrum. The IR spectra of the five compounds have many similar features corresponding to the common groups: P−O bands of the phosphonate in the region of 900−1200 cm^{-1}, the C−H bending and stretching bands at ca.1350 and 2950 cm^{-1}, respectively, and the broad O−H stretching bands of H_2O in the region of 3000−3500 cm^{-1}. Compounds **2** and **3** are isostructural; their spectra are almost identical. However, the spectrum of compound **4** is distinctly different from those of compounds **2** and **3** because of their completely different structures, although they possess similar compositions, which are in perfect agreement with their single-crystal X-ray analyses.

Photoluminescence Properties. The XRD powder patterns of compounds **1**−**5** are shown in Figure S1 in the Supporting Information. All the peaks of the five compounds can be indexed to their respective simulated XRD powder patterns, which indicates each of the five compounds is pure phase. The emission spectra of APD and compounds **1**−**5** in the solid state ($\lambda_{ex} = 300$ nm, slit width = 3 nm) at room temperature are depicted in Figure 11. As shown in Figure 11a, APD displays three intense emission peaks at 372, 396, and 469 nm and one shoulder peak at 516 nm; they are attributable to different intraligand transitions of APD, such as the $\pi \rightarrow \pi^*$, $\pi^* \rightarrow$ n, n $\rightarrow$ n*, and $\pi \rightarrow$ n transitions.[13] The emission spectra of compounds **1**−**5** are somewhat similar to that of discrete APD: the four emission peaks of discrete APD still appear, although some peaks are shifted a little (Figure 11b−f), which indicates those peaks in the spectra of compounds **1**−**5** are still caused by intraligand transitions of APD. [13] However, it is found that the relative intensities of the four peaks in the emission spectra of APD and compounds **1**−**5** are different (Figure 11), which indicates that the intraligand transitions of APD have been enhanced or weakened to different extents because of the introduction of different metal ions in the structures. The detailed mechanism is under investigation. Such phenomena are rarely reported in previous work, and the difference in the photoluminescence between the organic ligand and the metal−organic complex is usually caused by the metal ion-involved charge transfer (i.e., LMCT)[14] but not by the intraligand transition.

According to the single-crystal X-ray analyses, compounds **2** and **3** are isostructural, and their coordination environments and structures are similar; however, the relative intensities of their four emission peaks are distinctly different (Figure 11c and d), which indicates that the metal centers play important roles in the intraligand transitions of APD.

Under similar measurement conditions, when the excitation wavelengths range from 250 to 400 nm, the excitation wavelength was not found to change the emission peaks' positions and curve's shape for each of the six compounds. However, when excitation wavelength is longer, the excitation energy is lower and the overall emission intensity of each compound is lowered.

Conclusion

In summary, we hydrothermally synthesized five novel metal−APD complexes under similar conditions. The coexistence of the amino group and phosphonate groups makes APD exhibit zwitterionic (cationic and anionic) properties. At different pH values, different intramolecular H-bonds can be formed between its amino group and phosphonate groups, and APD exhibits different affinities for different metal ions. APD can act as a bi-, tri-, penta-, or heptadentate ligand in compounds **1**−**5**, and its hydroxyl group can be coordinated (in compounds **2**−**5**) or uncoordinated (in compound **1**) to the metal centers. On the basis of the different coordination modes of APD and different binuclear secondary building units (SBUs), the structures of compounds **1**−**5** span zero, one, two, and three dimensions.

The solid-state emission spectra of the five compounds have been measured, and their photoluminescence properties indicated that the introduction of different metal ions can enhance or weaken the intraligand transitions of APD.

Acknowledgment. This work was supported by the National Natural Science Foundation of China (Nos. 20271007, 20331010, and 90406002), and Specialized Research Fund for the Doctoral Program of Higher Education of China (No. 20030007014).

Supporting Information Available: Atomic coordinates, bond lengths and angles, thermal parameters and the solid-state emission spectra of compounds **1**−**5** at room temperature. This material is available free of charge via the Internet at http://pubs.acs.org.

IC052095H

---

(13) (a) Chen, W.; Wang, J. Y.; Chen, C.; Yue, Q.; Yuan, H. M.; Chen, J. X.; Wang, S. N. *Inorg. Chem.* **2003**, *42*, 944. (b) Wang, M. S.; Guo, G. C.; Fu, M. L.; Xu, L.; Cai, L. Z.; Huang, J. S. *Dalton Trans.* **2005**, 2899. (c) Chen, X. D.; Du, M.; Mak, T. C. W. *Chem. Commun.* **2005**, 4417.

(14) (a) Zhang, L. Y.; Liu, G. F.; Zheng, S. L.; Ye, B. H.; Zhang, X. M.; Chen, X. M. *Eur. J. Inorg. Chem.* **2003**, 2965. (b) Fu, Z. Y.; Wu, X. T.; Dai, J. C.; Hu, S. M.; Du, W. X.; Zhang, H. H.; Sun, R. Q. *Eur. J. Inorg. Chem.* **2002**, 2730.